Behavioral/Systems/Cognitive

Neural Correlates of Vibrotactile Working Memory in the Human Brain

Claudia Preuschhof,[1,2] Hauke R. Heekeren,[1,3] Birol Taskin,[1] Torsten Schubert,[2] and Arno Villringer[1]

[1]Berlin NeuroImaging Center and Department of Neurology, Charité – University Medicine Berlin, 10117 Berlin, Germany, [2]Department of Psychology, Humboldt University Berlin, 12489 Berlin, Germany, and [3]Max Planck Institute for Human Development, 14195 Berlin, Germany

Recent neurophysiological studies in macaques identified a network of brain regions related to vibrotactile working memory (WM), including somatosensory, motor, premotor, and prefrontal cortex. In these studies, monkeys decided which of two vibrotactile stimuli that were sequentially applied to their fingertips and separated by a short delay had the higher vibration frequency. Using the same task, the objective of the present study was to identify the neural correlates related to the different task periods (encoding, maintenance, and decision making) of vibrotactile WM in the human brain. For this purpose, we used event-related functional magnetic resonance imaging and contrasted WM trials with a control condition of vibrotactile stimulation that did not require maintenance and decision making. We found that vibrotactile WM has a similar but not identical neural organization in humans and monkeys. Consistent with neurophysiological data in monkeys and behavioral studies in humans, the primary somatosensory and the ventral premotor cortex exhibited increased activity during encoding. Maintenance of a vibrotactile memory trace evoked activity in the premotor and ventrolateral prefrontal cortex. Decision making caused activation in the somatosensory, premotor, and lateral prefrontal cortex. However, human vibrotactile WM recruited additional areas. Decision making activated a broader network than that studied thus far in monkeys. Maintenance and decision making additionally activated the inferior parietal lobe. Although the different task components evoked activity in distinctive neural networks, there was considerable overlap of activity, especially regarding maintenance and decision making, indicating that similar neural mechanisms are required for the subprocesses related to these task components.

Key words: **somatosensory; flutter vibration; delayed discrimination; working memory; decision making; fMRI**

Introduction

The ability to actively maintain representations of sensory information that is no longer available to the senses, flexibly update, and reorganize this information and use it for guiding actions or thoughts are essential parts of human behavior. These characteristics are subsumed under the psychological construct of working memory (WM), which is assumed to have a limited capacity and to operate in a time frame up to several seconds (Fuster, 2000; Levy and Goldman-Rakic, 2000). Baddeley's (2003) influential WM model proposes the existence of a central executive that controls information held in modality-specific storage systems. Like most of the research, this model focuses on visuospatial and phonological WM. However, for everyday behaviors such as manual object recognition or touch typing, WM for tactile features is an equally important capacity.

Using single-unit recordings in nonhuman primates, Romo and Salinas (2003) identified a network of brain regions related to vibrotactile WM. In these studies, monkeys had to decide which of two vibrations separated by a short delay had the higher frequency. Neurons in primary somatosensory cortex (S1), secondary somatosensory cortex (S2), prefrontal cortex (PFC), premotor cortex (PMC), and motor cortex show stimulus specificity (i.e., their firing rate increases parametrically with the vibration frequency, suggesting that they contain the neural representation of the vibrotactile stimuli). The neural code in PFC and PMC does not only directly represent the physical parameters of the vibrotactile stimulus during the delay but also encodes the difference between the two stimuli during the decision phase (Romo et al., 1999, 2004; Hernandez et al., 2002). These findings support the view that the lateral PFC and the PMC actively represent stimulus features required to perform the delayed discrimination.

Persistent neural activity in combination with stimulus specificity during a delay is the neural signature of WM (Goldman-Rakic, 1995). Persistent neural activity during vibrotactile WM was found in S2 during the early part of the delay, in PMC and PFC during the entire delay, but not in S1 (Romo et al., 1999, 2002, 2004; Hernandez et al., 2002). Contrary to the studies in monkeys, experiments using vibrotactile WM tasks in humans found indirect evidence for the contribution of S1 for maintaining the vibrotactile memory trace. In behavioral experiments, Harris et al. (2001) found that accuracy in the vibrotactile WM task decreases with the somatotopic distance between stimulated fingers and depends on delay length. Transcranial magnetic stim-

Received June 29, 2006; revised Nov. 3, 2006; accepted Nov. 3, 2006.

This study was supported by the Deutsche Forschungsgemeinschaft (Graduate Program "Neuropsychiatry and Psychology of Aging GRK 429") and the Bundesministerium für Bildung und Forschung (Berlin NeuroImaging Center). We thank Uwe Blücher and Raik Paulat for engineering the vibrotactile device and amplifier; Ruth Schubert, Christina Scheibe, and Yvonne Rothemund for comments on this manuscript; and Torsten Wüstenberg for technical help.

Correspondence should be addressed to Claudia Preuschhof, Berlin NeuroImaging Center, Charité – University Medicine Berlin, Charitéplatz 1, 10117 Berlin, Germany. E-mail: claudia.preuschhof@charite.de.

DOI:10.1523/JNEUROSCI.2767-06.2006

 0270-6474/06/2613231-09$15.00/0

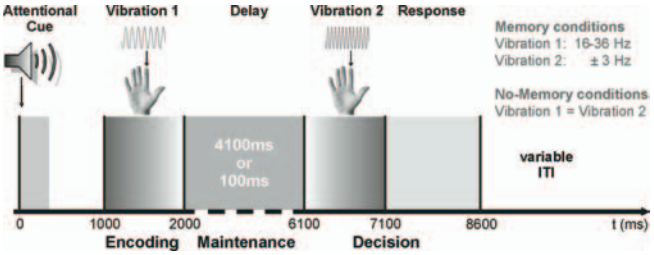

Figure 1. Experimental design. Subjects placed the tip of their right index finger on a rubber disk glued to a piezoelectric wafer. Each trial began with a warning tone for 100 ms. Nine-hundred milliseconds later, the first vibration was applied to the subject's finger, followed by a delay of 100 or 4100 ms. After the delay, the second vibration was applied. In the two Memory conditions, the subjects had to decide whether the second vibration had a higher or a lower frequency than the first vibration and indicated their choice by pressing one of two response buttons with the left index or left middle finger. The first vibration was one of six different frequencies (16, 20, 24, 28, 32, 36 Hz). The second vibration was either 3 Hz higher (50% of the trials) or lower than the first frequency. In two No-Memory conditions, the trial structure was kept constant, but both vibrations had the same frequency (one of the frequencies presented in the Memory conditions ranging from 13 to 39 Hz), and the subject only had to press one of the two buttons as soon as the second vibration appeared. ITI, Intertrial interval.

ulation of contralateral S1 impairs discrimination performance when applied during the early delay but not when applied during the later delay or ipsilaterally (Harris et al., 2002). These time-dependent somatotopical distance and laterality effects indicate that S1 is essential for building the vibrotactile memory trace and maintaining it during the early delay.

In the present study, we took advantage of event-related functional magnetic resonance imaging (fMRI) to study network activity related to vibrotactile WM in the healthy human brain. We used an event-related design to separate activity related to the different task periods: encoding, maintenance, and decision making.

Materials and Methods

Subjects. Twenty healthy volunteers (nine women; mean age, 26.9 years; age range, 22–34 years) participated in the study. All subjects were right-handed, had no structural brain abnormalities, and reported no history of neurological or psychiatric disorder. Handedness was assessed with the Edinburgh Handedness Inventory (Oldfield, 1971). All subjects were paid for participation and gave written informed consent before the experiment. The study was approved by the local Human Subjects Committee and adhered to the Human Subjects Guidelines of the Declaration of Helsinki.

Behavioral task. Subjects performed a vibrotactile delayed discrimination task (Fig. 1) similar to that previously used in primate studies (Romo et al., 1999) and human studies (Harris et al., 2002). In a series of behavioral experiments, we determined the optimal range of vibration frequencies, frequency difference between the first and the second vibration, and length of the delay period for the fMRI study. In the present fMRI experiment, each trial began with a warning tone for 100 ms, indicating that the next pair of vibrations would appear. Nine hundred milliseconds later, the first vibration was applied to the subject's right index finger pad followed by a delay of 100 ms (Short-Delay-Memory trial) or 4100 ms (Long-Delay-Memory trial). After the delay, the second vibration was applied to the right index finger. The subjects had to decide whether the second vibration had a higher or a lower frequency than the first vibration and to indicate their choice by pressing one of two response buttons with the left index or left middle finger, respectively. All vibrations lasted 1000 ms. Maximum response time (RT) was 2600 ms measured from the start of the second vibration. The first vibration was one of six different frequencies (16, 20, 24, 28, 32, 36 Hz). The second vibration was either 3 Hz higher (50% of the trials) or lower than the first frequency. In two No-Memory conditions comprising Short-Delay-No-Memory and Long-Delay-No-Memory trials, the trial structure was kept constant, but both vibrations had the same frequency (one of the frequencies presented in the Memory-runs ranging from 13 to 39 Hz), and the subject only had to press one of the two buttons as soon as the second vibration appeared. For both conditions, subjects were instructed to keep their eyes closed during the functional runs and to respond as accurately and quickly as possible. Memory and No-Memory conditions were presented in separate runs with two to three Memory and three No-Memory runs. Before scanning, subjects completed a Memory practice run outside of the scanner in which they received visual feedback regarding their performance. The order and temporal sequence of the trials in each run was optimized and pseudorandomized using Optseq2 (http://surfer.nmr.mgh.harvard.edu/optseq). Each run lasted 8 min 45 s and contained 24 short trials as well as 24 long trials. One-third of the scanning time consisted of null events that were randomly inserted between trials. Trial onsets were jittered in steps of 0.5 repetition time (TR) (500 ms).

Materials and stimuli. Vibrations were produced using a piezoelectric wafer (length, 31 mm; width, 9.6 mm; thickness, 0.65 mm; model PL-127.251, PI Ceramic, Lederhose, Germany) driven by sinusoidal 2.5–60 V pulses from a custom-built amplifier. A flat semicircle-shaped rubber pad (diameter, 13 mm) was glued on the top surface at the outer end of the wafer. The wafer was placed in a plastic box (length, 48 mm; width, 31 mm; thickness, 6 mm) with only the rubber pad exposed outwards making contact with the subject's skin. During the experiment, the plastic box was positioned on a foam arm rest and secured with adhesive tape to the subject's finger. Vibration frequencies varied between 13 and 39 Hz. The amplitude of the vibrations was ~450 μm. Five hundred Hertz warning tones were presented via headphones. Experimental stimulation and response registration was controlled by a computer running Presentation (version 0.8.1; Neurobehavioral Systems, Albany, CA).

fMRI scanning. Imaging was conducted on a 1.5 T Magnetom Sonata MRI system (Siemens, Erlangen, Germany) equipped with a standard head coil. A vacuum pad was used to minimize head motion. Functional images were acquired using a BOLD (blood oxygenation level-dependent)-sensitive T2*-weighted echo-planar imaging (EPI) sequence [TR, 2500 ms; echo time (TE), 40 ms; flip angle, 90°; field of view, 256 mm; matrix, 64 × 64 mm; 26 axial slices approximately parallel to the bicommissural plane; slice thickness, 4 mm; interleaved acquisition). Four or five functional runs of 210 volumes each were acquired. The first two scans of each run were discarded to allow longitudinal magnetization to reach equilibrium. After the functional runs, structural images were collected using a T1-weighted MP-RAGE (three-dimensional magnetization prepared rapid acquisition gradient echo) sequence (TR, 2.73 ms; TE, 3.93 ms; flip angle, 7°; 176 sagittal slices; voxel size, 1 × 1 × 1 mm).

Behavioral data analysis. Behavioral data were analyzed using SPSS (version 12.0; SPSS, Cary, NC). RT in milliseconds and accuracy in relative frequency of correct responses were computed for each condition and subject. Repeated-measures ANOVAs with the within-subject factors condition and delay as well as the random factor subjects were conducted on RT and accuracy.

fMRI data analysis. MRI data were analyzed with SPM2 (http://www.fil.ion.ucl.ac.uk/spm/software/spm2). Preprocessing of the data was performed before statistical evaluation. First, slice timing differences resulting from acquisition order were adjusted. Parameters for motion artifacts were determined using six parameters for rigid body transformation and translation. The first image of the first run was normalized to the Montreal Neurological Institute (MNI) EPI-template. The parameters from this normalization and the motion correction were applied to all functional images. Finally, data were spatially smoothed using a three-dimensional Gaussian filter of 8 mm full-width at half-maximum.

Voxel-based statistical analysis was based on the General Linear Model (Friston et al., 1995). Low-frequency drifts were removed using a temporal high-pass filter (cutoff, 128 s), and intrinsic autocorrelations were modeled. Design matrices were generated using event-related regressors and then convolved with a canonical hemodynamic response function. Error trials included incorrect trials and no-response trials and were modeled as regressors of no interest.

In a first model, we assessed activity related to the different task periods of the vibrotactile WM task. We specified a model using eight regressors representing encoding, maintenance, decision making, and error trials

Table 1. Behavioral data

	Memory		No memory	
	Short delay	Long delay	Short delay	Long delay
Accuracy	0.78 ± 0.02	0.74 ± 0.02	0.99 ± 0.01	0.98 ± 0.01
Response times	1124.68 ± 61.75	1152.41 ± 66.68	364.93 ± 37.48	359.49 ± 32.38

Accuracy as relative number of correct responses and response times in milliseconds are presented for the four experimental conditions, Short-Delay-Memory trial, Long-Delay-Memory trial, Short-Delay-No-Memory trial, and Long-Delay-No-Memory trial, including SEM.

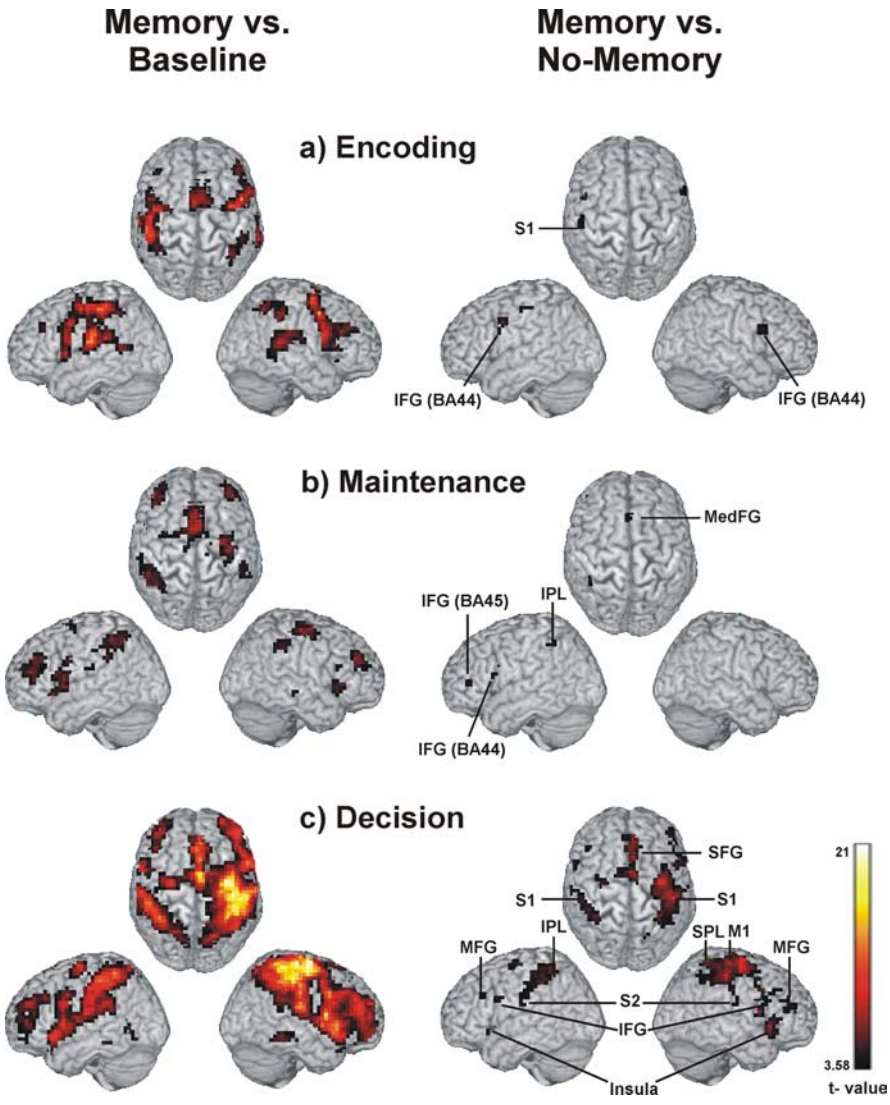

Figure 2. Activation related to the different task periods. Network of brain regions related to vibrotactile delayed discrimination using the contrast Memory-condition > Baseline (left) and network of brain regions related specifically to vibrotactile working memory using the contrast Memory condition > No-Memory condition (right) for the different task periods. ***a***, Encoding. ***b***, Maintenance. ***c***, Decision. Activation clusters ($p < 0.001$, uncorrected) up to a depth of 15 mm are projected to the cortical surface of the MNI template "Colin." M1, Primary motor cortex; MedFG, medial frontal gyrus.

for the two memory conditions, respectively. The regressor for encoding comprised the duration of the first vibration and lasted 1 s. The regressor for maintenance started 100 ms after the end of the first vibration and lasted 4 s. The regressor for decision making started with the beginning of the second vibration and lasted 1.5 s, including the subject's response. Whereas the regressor for maintenance only included the 4-s-long maintenance period of the Long-Delay trials, the regressors for encoding and decision making incorporated both Long-Delay and Short-Delay trials. The regressor for the error trials started with the beginning of the first vibration and lasted until 1.5 s after the beginning of the second vibration. To obtain group activation maps, contrast images were computed for all Memory versus baseline (null events) and all Memory versus No-Memory conditions for each subject using *t* statistics.

To compare brain regions related to vibrotactile WM with short and long delay periods, an additional model was specified using six regressors. These regressors were related to Short-Delay trials, Long-Delay trials, and error trials for the two memory conditions. All regressors in this model started with the onset of the first vibration and lasted until 1.5 s after the onset of the second vibration totaling 2.6 s for the Short-Delay trials and 6.6 s for the Long-Delay trials. Contrast images were then computed for the Short-Delay-Memory versus Short-Delay-No-Memory condition and the Long-Delay-Memory versus Long-Delay-No-Memory condition. Contrast images were entered into mixed-effects analyses to obtain group activation maps. For illustration purposes, both activation patterns were then projected onto the same cortical surface.

The significance threshold for all mixed-effects analyses was set to $t \geq 3.58$ ($p < 0.001$; uncorrected for multiple comparisons). Only activation clusters with a minimum cluster size of five continuous voxels are reported.

Time courses for the hemodynamic responses were computed using MarsBaR 0.38 (https://sourceforge.net/projects/marsbar). For each subject, we computed finite impulse response models for the peak voxels that were significantly activated for the three different task periods (encoding, maintenance, and decision making) in the contrast Memory versus No-Memory. The regressor for the finite impulse response model started with the onset of the tone and lasted 7.6 s. Percentage signal change was estimated at each of 10 time points with an interval of 2.5 s ranging from trial onset to 25 s posttrial onset for Long-Delay-Memory and Long-Delay-No-Memory trials, respectively. For the single time bins, paired *t* tests comparing both memory conditions were computed.

We additionally computed percentage signal change related to the single task periods using finite impulse response functions to model each task period. Otherwise, the regressors for this analysis (encoding, delay, decision making, and error trials) were identical to the event-related analysis described above. Paired *t* tests comparing both memory conditions were computed for each task period.

Results

Behavioral data

Behavioral data are shown in Table 1. The factor condition had a significant effect on accuracy with worse performance in the Memory compared with the No-Memory conditions ($F(1,19) = 140.58$; $p < 0.001$). The factor delay also showed a significant effect on accuracy with lower accuracy for the long delay periods ($F(1,19) = 6.01$; $p < 0.05$). Additionally, there was a trend toward an interaction between condition and delay ($F(1,19) = 4.3$; $p < 0.055$) indicating that mainly the difference between the two Memory conditions ($t(19) = 2.3$; $p < 0.05$) contributed to the effect of delay. Response times (RT) differed only with regard to memory condition and were higher in the Memory compared with the No-Memory conditions ($F(1,19) = 127.47$; $p < 0.001$). Neither the effect of delay ($F(1,19) = 0.78$; $p = 0.39$) nor the

interaction between condition and delay ($F(1,19) = 3.41$; $p = 0.08$) was significant for the RT.

fMRI data

Main effect of vibrotactile discrimination (Memory vs Baseline)

The left panel of Figure 2 shows the activation pattern for the encoding, maintenance, and decision period for the Memory condition compared with baseline.

Encoding elicited increased activity in the contralateral S1 [Brodmann Area 2 (BA2)] and M1 (primary motor cortex) and bilaterally in S2 (BA43). Bilateral activation was also found in the inferior parietal lobe (IPL) (BA40), the superior temporal gyrus (BA22/37), the anterior insular cortex (BA13), the precentral and posterior inferior frontal gyrus (IFG) (BA6/44), supplementary motor area (SMA) (BA6), the middle frontal gyrus (MFG) (BA46), striatum, and thalamus.

Maintenance resulted in increased activity in bilateral inferior parietal lobe (IPL) (BA40), anterior insular cortex (BA13), precentral gyrus and IFG (BA6/44), MFG (BA46), SMA, anterior cingulate cortex, and striatum as well as left S2 (BA43) and right middle temporal gyrus (BA21).

Decision making was associated with the most widespread activation, including bilateral S1 (BA2), S2 (BA40/43), inferior and superior parietal lobe (BA40, BA7), superior temporal gyrus (BA22/37), primary and premotor cortex (BA4, BA6, BA8), MFG (BA46), IFG (BA44/47), anterior insular cortex (BA13), thalamus, and striatum.

Table 2. Anatomical locations and MNI coordinates for the contrast Memory > No-Memory condition for encoding, maintenance, and decision

Condition	Cluster size	Anatomical region	BA	Hemisphere	MNI coordinates *x*	*y*	*z*	Voxel *t* value
Encoding	28	IFG	44	L	−48	4	36	6.29
	8	Postcentral G	2 (SI)	L	−56	−28	52	4.68
	20	IFG	44	R	56	12	24	4.68
Maintenance	39	IPL	40	L	−32	−48	44	5.64
	11	IFG	44	L	−44	12	24	4.99
	5	IFG	45	L	−44	40	4	4.71
	15	MedFG	8	L	−8	28	44	4.44
Decision	334	SFG	6	R	8	−4	56	10.14
		MedFG	8	R	4	32	44	9.22
		A Cing G	32	L	−8	16	44	6.84
		M Cing G	24	R	8	4	40	6.13
	445	Precentral G	6	R	36	−12	60	9.68
		Postcentral G	2 (SI)	R	48	−28	52	9.33
		IPL	40	R	36	−48	40	6.97
		SPL	7	R	36	−48	68	6.62
	112	Striatum		R	8	4	8	8.13
	118	A Ins C	13	R	44	20	−4	7.59
	57	Precentral G	44	R	60	8	12	7.35
		IFG	44/45	R	56	12	36	5.45
	169	IPL	40	L	−44	−36	44	7.19
		Postcentral G	2	L	−64	−24	32	4.60
	50	A Ins C	13	L	−36	20	0	6.45
	5	Precuneus	7	R	16	−68	52	5.54
	11	Postcentral G	43 (SII)	R	48	−20	20	5.49
	22	Precentral G	6	L	−32	−12	64	5.34
	12	Striatum		L	−16	8	12	5.17
	6	Thalamus		R	8	−20	4	5.04
	25	MFG	46	R	44	40	20	4.88
	9	IFG	44	L	−56	8	28	4.37
	7	MFG	46	L	−48	24	28	4.25

$p < 0.001$. A, Anterior; C, cortex; Cing, cingulate; F, frontal; G, gyrus; I, inferior; Ins, insular; L, lobe; M, middle; Med, medial; P, parietal; S, superior.

The comparison of the Memory condition to Baseline showed that our vibrotactile stimulus is capable of reliably activating the somatosensory network. The activation pattern is similar to other studies using vibrotactile stimuli and tasks requiring attention (Staines et al., 2002; Nelson et al., 2004). Passive vibrotactile stimulation, in contrast, causes activity restricted to somatosensory regions (Burton et al., 1993).

Differential effect of vibrotactile WM (Memory vs No-Memory)

Because we were interested in the specific brain regions involved in vibrotactile WM, WM trials were compared with trials not requiring WM to control for unspecific somatosensory and motor activity. We are aware of the known criticism of the method of cognitive subtraction in neuroimaging studies, which relies on the assumption of "pure insertion" (for a critical discussion of this issue, see Friston et al., 1996). However, in any case, the present subtraction approach should uncover those specific regions that are more strongly activated in the Memory compared with the No-Memory condition because of the involved WM component.

Table 2 contains the activation peaks for the encoding, maintenance, and decision period (i.e., for the Memory compared with No-Memory condition). During encoding, the left S1 (BA2) and bilateral posterior IFG (BA44/45) showed increased activity (Fig. 2*a*, right panel). Maintenance was related to a left lateralized network including the IPL (BA40), the ventral PMC in the posterior IFG (BA44), the ventrolateral PFC (VLPFC) in the anterior IFG (BA45), and the medial PMC in the medial frontal gyrus (BA8) (Fig. 2*b*, right panel). In the decision period, a distributed network including bilateral SMA (BA6/8) extending to the cingulate gyrus (BA24/32), precentral gyrus (BA6), IFG (BA44/45), and the dorsolateral PFC (DLPFC) in the MFG (BA9/46) showed increased activity. This phase also led to increased activity in bilateral S1 (BA1/2) and S2 (BA43), IPL (BA40), anterior insular cortex (BA13), and striatum. The right precuneus (BA7) and thalamus also showed increased activity during decision making (Fig. 2*c*, right panel).

To verify that the brain regions related to maintenance sustained their activity during the entire delay period, we computed the hemodynamic response time courses for the brain regions that exhibited significantly higher activity in the Memory compared with the No-Memory condition. As shown in Figure 3 (top and middle panels), the regions showing delay-related activity (i.e., ventral PMC, medial PMC, VLPFC, and IPL) started to exhibit increased activity compared with the No-Memory condition approximately with the onset of the delay period and sustained this increased activity level during the entire delay period. To determine the specificity of this sustained activity for the delay-related brain regions, we also calculated the time courses for peak voxels in S1, which showed significantly increased activity during encoding as well as for peak voxels in the precentral gyrus, which was significantly activated during decision making. S1 activity was increased in the Memory compared with the No-Memory condition during the early part of the trial when the first vibrotactile stimulus had to be encoded and then again around the time when the second vibrotactile stimulus was applied. The premotor area of the precentral gyrus only exhibited significantly

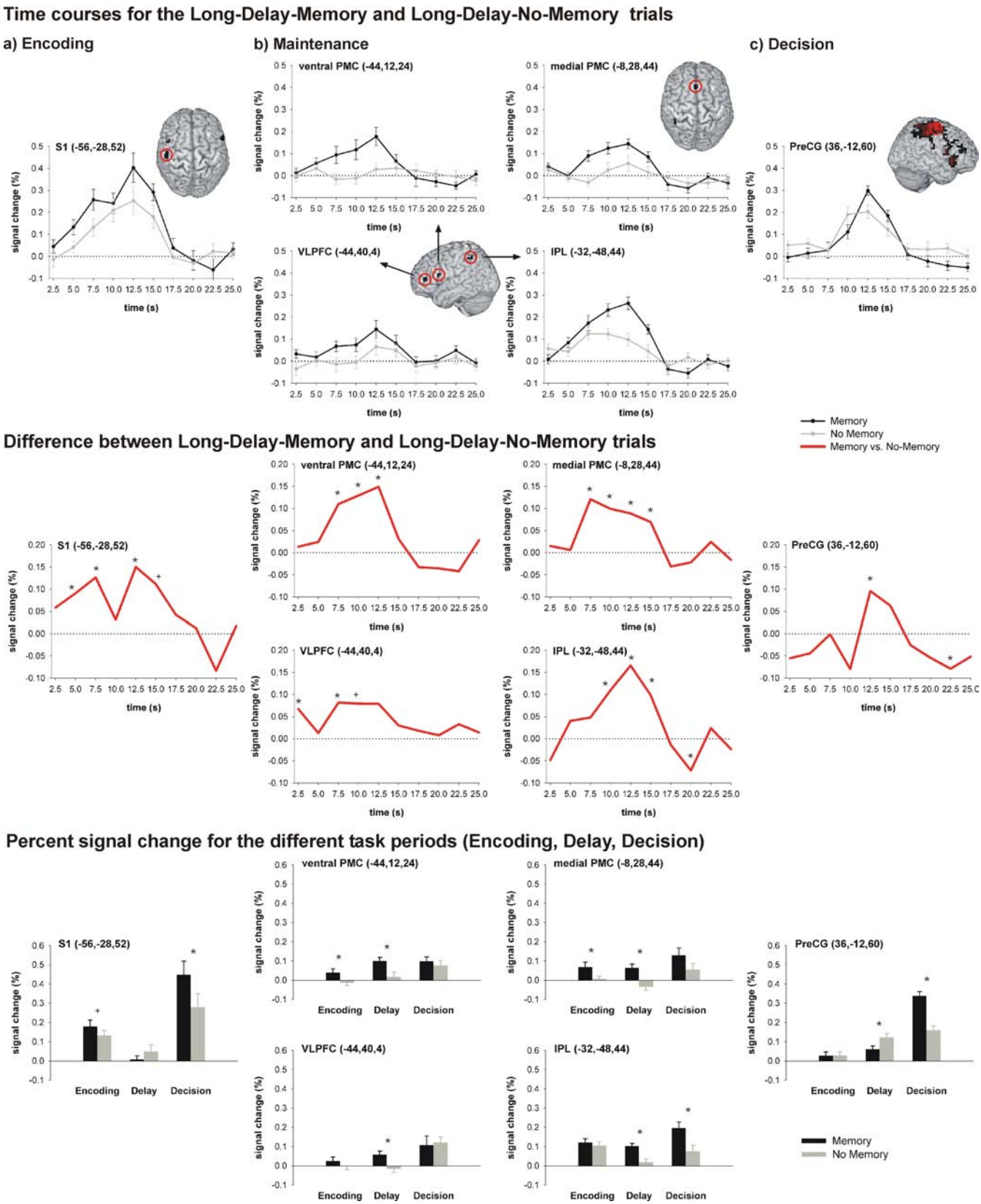

Figure 3. Time courses for the Long-Delay trials and percentage signal change for the different task periods. Top, ***a***, Time courses for the S1 peak voxel that exhibited increased activity during encoding. ***b***, Time courses for the peak voxels of the four regions that exhibited significantly higher activity during the delay period (medial PMC, ventral PMC, VLPFC, IPL). ***c***, Time course of the peak voxel in the precentral gyrus that exhibited increased activity during the decision phase. Middle, Difference between the time courses for the Long-Delay-Memory and the Long-Delay-No-Memory trials for the same peak voxels. Bottom, Percentage signal change for the different task periods (Encoding, Delay, Decision) for the same peak voxels. Error bars indicate SEM. Significant differences ($p < 0.05$) between both conditions are indicated by asterisks; trends ($0.063 < p < 0.05$) are indicated by plus symbols. PreCG, Precentral gyrus.

increased activity in the Memory compared with the No-Memory condition during the late segment of the time course corresponding to the decision period.

To get a more detailed picture of how the activity in the same six peak voxels (ventral PMC, medial PMC, VLPFC, IPL, S1, and precentral gyrus) differed with regard to the different periods of the vibrotactile WM task, we additionally calculated percentage signal change related to the different task periods (Fig. 3, bottom panel). This analysis revealed that activity in S1 is not enhanced and does not significantly differ between the Memory and the No-Memory conditions during the delay period. In contrast, the activity in the ventral and medial PMC, in the VLPFC and the IPL is enhanced and significantly differs between both conditions during the delay. The precentral gyrus shows significantly higher activity in the Memory compared with the No-Memory condition only in the decision period.

Effect of delay (during Memory trials vs No-Memory trials)

Figure 4 depicts the localization of activation in the Short-Delay-Memory and Long-Delay-Memory trials. A similar network was activated during Short-Delay-Memory and Long-Delay-Memory trials compared with the respective control conditions, including IPL (BA40), MFG (BA9/46), IFG (BA44/45), and medial PMC (BA8) (Table 3).

Although Long-Delay trials had more anterior activation peaks in the lateral PFC and recruited the posterior parietal cortex (PPC), the opposite pattern was found for Short-Delay trials. Short-Delay trials caused more posterior activation of the lateral PFC extending into premotor areas, whereas the parietal activation extended into S1. This indicates that WM for extremely short delays relies more on sensory regions and PMC compared with WM for longer delays. The latter seems to rely on anterior lateral PFC and PPC, areas that can maintain stimuli for several seconds. In the visual modality, a similar activation gradient has been observed (Cornette et al., 2002).

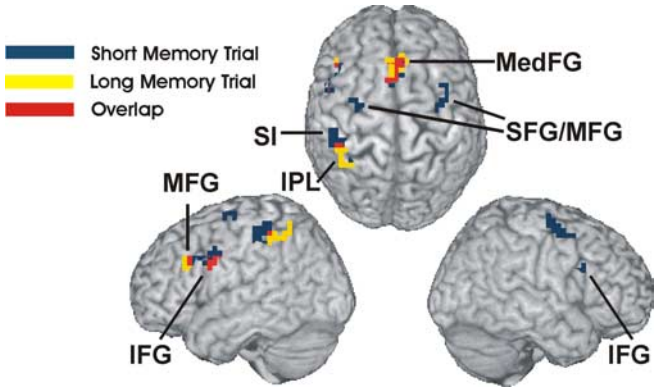

Figure 4. Activation of Short- and Long-Delay-Memory trials. Brain regions activated during the Short-Delay-Memory trial > Short-Delay-No-Memory trial (blue) and Long-Delay-Memory trial > Long-Delay-No-Memory trial (yellow). Although there is considerable overlap (shown in red) between both conditions, Long-Delay-Memory trials activate more anterior parts of the lateral prefrontal cortex and more posterior parts of the parietal cortex. Short-Delay-Memory trials show the reverse pattern and activate more posterior parts of the lateral prefrontal cortex extending to premotor areas and more anterior parts of the parietal cortex extending to S1. Activation clusters ($p < 0.001$, uncorrected) up to a depth of 15 mm are projected to the surface of the MNI template "Colin." MedFG, Medial frontal gyrus.

Table 3. Anatomical locations and MNI coordinates for the contrasts Short-Delay-Memory trial > Short-Delay-No-Memory trial and Long-Delay-Memory trial > Long-Delay-No-Memory trial

			Short-Delay-Memory trial				Long-Delay-Memory trial			
			MNI coordinates				MNI coordinates			
Anatomical region	BA	Hemisphere	*x*	*y*	*z*	Voxel *t* value	*x*	*y*	*z*	Voxel *t* value
Postcentral G	2	L	−52	−28	52	5.59				
IPL	40	L	−48	−40	56	5.78	−44	−44	44	8.64
SPL	7	L					−36	−56	60	4.60
MedFG	8	L/R	4	24	44	6.15	0	24	48	6.18
MFG/ SFG	6	L	−24	−12	56	4.44				
		R	36	−4	56	5.40				
MFG	9/46	L	−44	24	32	4.88	−48	24	28	4.76
IFG	44	L	−48	4	32	7.33	−48	4	32	5.47
		R	48	12	24	4.94				
Striatum		R	16	16	0	4.74				

$p < 0.001$. A, Anterior; C, cortex; Cing, cingulate; F, frontal; G, gyrus; I, inferior; Ins, insular; L, lobe; M, middle; Med, medial; P, parietal; S, superior; T, temporal.

Discussion

The goal of the present study was to identify brain regions related to the different periods of a vibrotactile WM task in humans.

Encoding a vibrotactile stimulus into WM compared with the No-Memory condition activated S1. Similarly, S1 neurons in the macaque brain show higher firing rates during discrimination than during passive vibrotactile stimulation (Salinas et al., 2000). Furthermore, even when vibrotactile stimulation is substituted by direct electrical stimulation of S1, monkeys correctly perform the delayed discrimination (Romo et al., 2000). Therefore, the neural code in S1 seems sufficient to generate the vibrotactile memory trace necessary to perform the task. Our data suggest that in the human brain, S1 neurons are also crucial for encoding the vibration frequency, complementing findings by Harris et al. (2001, 2002).

Encoding additionally recruited the posterior IFG (BA44). There is evidence that BA44 is homologous to the macaque area F5 corresponding to the ventral PMC (Rizzolatti et al., 2002). Although Romo et al. (2004) found encoding-related activity in F5, the ventral PMC does not seem to be crucial for encoding the vibrotactile memory trace in monkeys. The human posterior IFG exhibits increased activity during active compared with passive vibrotactile stimulation (Hagen et al., 2002). IFG is important for encoding visual and phonological information (Floel et al., 2004; Kahn et al., 2005). Also, divided attention during encoding leads to memory deficits and affects activity in IFG (Anderson et al., 2000). Together with the finding that attention modulates activity in S1 (Roland, 1981), these results suggest that the posterior IFG might be involved in the allocation of attentional resources required for successful encoding of the vibrotactile stimulus in S1.

Given the fact that the left BA44 (i.e., Broca's area) plays an important role in language processing (Smith et al., 1998; Friederici, 2002), it is also possible that this activation reflects verbal encoding strategies used by our subjects. Alternatively, Schubotz et al. (2003) and Schubotz and von Cramon (2001) suggested that the ventral PMC might be related to the processing of temporal patterns independent of modality. Our finding that processing the frequency of vibrotactile stimuli activates the same brain region supports this view and implies that it extends to the tactile modality.

Maintaining the vibrotactile memory trace was accompanied by increased activation in the medial (BA8) and ventral (BA44) PMC, VLPFC (BA45), and IPL (BA40). These results correspond

with results of electrophysiological studies demonstrating that neurons in the medial PMC, ventral PMC, and VLPFC represent information about the vibration frequency during the delay (Romo et al., 1999, 2004; Hernandez et al., 2002).

Stimulus-selective persistent delay activity can be regarded as the neurophysiological correlate of WM (Goldman-Rakic, 1995). Although the lateral PFC seems to be crucial for WM, its role for the maintenance of information is still under debate (Curtis and D'Esposito, 2003; Postle, 2006). Furthermore, it remains unclear what stimulus-selective persistent activity in the lateral PFC reflects. Some authors disagree with the view that stimulus representations are maintained in the lateral PFC and assume that persistent activity in this area reflects processes assisting in maintenance such as top-down control (Miller, 2000), attentional (Lebedev et al., 2004), or response selection (Rowe and Passingham, 2001). According to this view, maintenance is instead supported by a parietopremotor cortical network (Rowe et al., 2000; Sakai et al., 2002; Manoach et al., 2003) and modality-specific sensory and association areas (Pasternak and Greenlee, 2005). However, we found increased activation in the VLPFC during maintenance in a vibrotactile WM task with a low WM load and minimal executive processing demands. Similarly, neurons in the inferior convexity of the macaque brain show stimulus-selective activity throughout the delay (Romo et al., 1999). This finding is consistent with theories that the lateral PFC shows a material-specific organization with maintenance of nonspatial information related to VLPFC (Levy and Goldman-Rakic, 2000; Courtney, 2004).

Medial and ventral PMC have been associated with sensory-motor transformation, sensory guided movement selection, and preparation (Wise et al., 1997; Rizzolatti and Luppino, 2001). Whereas the lateral PFC seems to support both sensory- and motor-related aspects of WM, sustained activity in the PMC seems to be more closely related to motor behavior.

IFG, medial PMC, and ventral PMC have been associated with subvocal rehearsal of phonological information (Smith et al., 1998) and with WM for auditory pitch (Zatorre et al., 1994; Gaab et al., 2003). Therefore, the activation of these areas in our study could be related to verbal or vocal rehearsal strategies. An alternative interpretation is that the activation of these brain regions reflects the fact that verbal, auditory, and vibrotactile stimuli rely on the processing of temporal patterns and might therefore recruit a common neural network.

We found evidence for the involvement of the IPL in maintenance during vibrotactile WM, a region that has not been associated with vibrotactile WM before. However, the IPL receives extensive projections from the somatosensory cortex (Kaas, 1993), and cells in IPL exhibit sustained delay activity in visual WM tasks (Constantinidis and Steinmetz, 1996; Tsutsui et al., 2003). The lateral PFC and the PMC are connected with the IPL (Petrides and Pandya, 1984). Altogether, the four regions activated during maintenance receive projections from the somatosensory cortex or somatosensory association areas, exhibit stimulus-specific sustained activity, and are interconnected. This suggests that these regions provide the neural substrate necessary for maintaining the vibrotactile memory trace during the delay.

We did not detect increased activity in the somatosensory cortex during the 4-s-long delay period. Harris et al. (2001, 2002) found indirect evidence for the importance of S1 during the early delay in human vibrotactile WM. Although studies in nonhuman primates also failed to find evidence for S1 activity during the retention interval (Romo and Salinas, 2003), they have reliably observed activity, albeit relatively short-lived in S2 (Salinas et al., 2000).

To resolve these inconsistent findings, we compared the activation related to Long- and Short-Delay-Memory trials. Consistent with the event-related analysis, the Long-Delay trials were not associated with significantly increased activity in S1. However, the Short-Delay trials were accompanied by increased activity in S1. Because Short- and Long-Delay trials are intermingled and the subject never knew what to expect, S1 activity should not differ between both conditions within the first 100 ms of the delay. Therefore, our data indirectly suggest that S1 maintains the vibrotactile memory trace during the early delay (in both conditions), corroborating the data by Harris et al. (2001, 2002). With respect to S2, our data do not indicate an involvement of S2 in maintaining the vibrotactile memory trace in humans and thus is not in line with evidence from monkeys.

However, because activity in S1 and S2 may not persist during the entire 4 s delay in the Long-Delay trials, it may not have enough power to reach statistical significance in the Long-Delay trials (acknowledging the general fact that a lack of a statistically significant increase in activity does not exclude that a smaller or transient increase in activity escaped the threshold for statistical significance). Although the above mentioned explanation is plausible, we are cautious to claim that our data can finally resolve this issue. To disentangle activity on a time scale of 100 ms is pushing the fMRI approach to its limits. Additional studies, potentially involving simultaneous EEG-fMRI technology (Thees et al., 2003), seem warranted to finally clarify this issue.

Decision making was accompanied by activation of medial PMC, lateral PMC, and lateral PFC. Cells in these regions also show decision-related responses in the studies of vibrotactile WM in macaques (Romo et al., 1999, 2004; Hernandez et al., 2002). Additionally, the decision period caused bilateral activation of the IPL. The PPC has been associated previously with sensory-motor integration and motor intentions (Andersen and Buneo, 2002). It is connected with motor areas of the frontal lobe, receives somatosensory input (Petrides and Pandya, 1984), and might therefore play a prominent role in the formation of the decision and its transfer to the motor areas of the frontal lobe. In a visual direction-discrimination task, similar brain regions, including the frontal eye field and the lateral intraparietal area in the PPC, exhibited decision-related activity (Kim and Shadlen, 1999; Shadlen and Newsome, 2001). These brain regions accumulate information about motion direction fed forward from the motion-sensitive medial temporal area (MT) (Ditterich et al., 2003).

We also found increased activity in S1 and S2 during the decision period, which is probably related to the processing of the second vibration. Also, these somatosensory regions might play a role that is analogous to area MT in the visual domain by representing the sensory evidence necessary to generate the decision. S2 exhibited decision-related responses in monkeys during vibrotactile WM but later than PMC and lateral PFC, indicating that this region does not actively participate in forming the decision (Romo et al., 2004). Decision making also involved bilateral activation of the anterior insula and the striatum. These regions are related to processes supporting decision making such as long-term memory (Friedman et al., 1986) and reward processing (Schultz, 2000).

PFC, PMC, and IPL showed increased activity during maintenance and decision making. This is compatible with computational models, suggesting that both processes are related to similar neural mechanisms requiring persistent activity (Mazurek et al., 2003; Machens et al., 2005; Miller and Wang, 2006). Stimulus-selective persistent activity during WM delays has been shown for lateral PFC (Sawaguchi and Yamane, 1999) and PPC (Constantinidis and Steinmetz, 1996). The DLPFC is involved in decision making in humans and nonhuman primates (Kim and Shadlen,

1999; Heekeren et al., 2004, 2006). In addition, Huk and Shadlen (2005) showed that decision-related activity in the PPC reflects the temporal integration of sensory evidence over time, a mechanism that requires short-term memory and, therefore, persistent neural activity.

Together, this is the first neuroimaging study to describe the neural correlates of vibrotactile WM in the human brain and to demonstrate a similar organization of vibrotactile WM in humans and moneys. However, we found that human vibrotactile working memory involved additional areas. Our findings support the view that complementary experiments in humans and monkeys help to elucidate the cerebral organization of cognitive functions in the primate brain.

References

Andersen RA, Buneo CA (2002) Intentional maps in posterior parietal cortex. Annu Rev Neurosci 25:189–220.

Anderson ND, Iidaka T, Cabeza R, Kapur S, McIntosh AR, Craik FI (2000) The effects of divided attention on encoding- and retrieval-related brain activity: a PET study of younger and older adults. J Cogn Neurosci 12:775–792.

Baddeley A (2003) Working memory: looking back and looking forward. Nat Rev Neurosci 4:829–839.

Burton H, Videen TO, Raichle ME (1993) Tactile-vibration-activated foci in insular and parietal-opercular cortex studied with positron emission tomography: mapping the second somatosensory area in humans. Somatosens Mot Res 10:297–308.

Constantinidis C, Steinmetz MA (1996) Neuronal activity in posterior parietal area 7a during the delay periods of a spatial memory task. J Neurophysiol 76:1352–1355.

Cornette L, Dupont P, Orban GA (2002) The neural substrate of orientation short-term memory and resistance to distractor items. Eur J Neurosci 15:165–175.

Courtney SM (2004) Attention and cognitive control as emergent properties of information representation in working memory. Cogn Affect Behav Neurosci 4:501–516.

Curtis CE, D'Esposito M (2003) Persistent activity in the prefrontal cortex during working memory. Trends Cogn Sci 7:415–423.

Ditterich J, Mazurek ME, Shadlen MN (2003) Microstimulation of visual cortex affects the speed of perceptual decisions. Nat Neurosci 6:891–898.

Floel A, Poeppel D, Buffalo EA, Braun A, Wu CW, Seo HJ, Stefan K, Knecht S, Cohen LG (2004) Prefrontal cortex asymmetry for memory encoding of words and abstract shapes. Cereb Cortex 14:404–409.

Friederici AD (2002) Towards a neural basis of auditory sentence processing. Trends Cogn Sci 6:78–84.

Friedman DP, Murray EA, O'Neill JB, Mishkin M (1986) Cortical connections of the somatosensory fields of the lateral sulcus of macaques: evidence for a corticolimbic pathway for touch. J Comp Neurol 252:323–347.

Friston KJ, Holmes AP, Worsley KJ, Poline J-P, Frith CD, Frackowiak RSJ (1995) Statistical parametric maps in functional imaging: a general linear approach. Hum Brain Mapp 2:189–210.

Friston KJ, Price CJ, Fletcher P, Moore C, Frackowiak RS, Dolan RJ (1996) The trouble with cognitive subtraction. NeuroImage 4:97–104.

Fuster JM (2000) Executive frontal functions. Exp Brain Res 133:66–70.

Gaab N, Gaser C, Zaehle T, Jancke L, Schlaug G (2003) Functional anatomy of pitch memory–an fMRI study with sparse temporal sampling. NeuroImage 19:1417–1426.

Goldman-Rakic PS (1995) Cellular basis of working memory. Neuron 14:477–485.

Hagen MC, Zald DH, Thornton TA, Pardo JV (2002) Somatosensory processing in the human inferior prefrontal cortex. J Neurophysiol 88:1400–1406.

Harris JA, Harris IM, Diamond ME (2001) The topography of tactile working memory. J Neurosci 21:8262–8269.

Harris JA, Miniussi C, Harris IM, Diamond ME (2002) Transient storage of a tactile memory trace in primary somatosensory cortex. J Neurosci 22:8720–8725.

Heekeren HR, Marrett S, Bandettini PA, Ungerleider LG (2004) A general mechanism for perceptual decision-making in the human brain. Nature 431:859–862.

Heekeren HR, Marrett S, Ruff DA, Bandettini PA, Ungerleider LG (2006) Involvement of human left dorsolateral prefrontal cortex in perceptual decision making is independent of response modality. Proc Natl Acad Sci USA 103:10023–10028.

Hernandez A, Zainos A, Romo R (2002) Temporal evolution of a decision-making process in medial premotor cortex. Neuron 33:959–972.

Huk AC, Shadlen MN (2005) Neural activity in macaque parietal cortex reflects temporal integration of visual motion signals during perceptual decision making. J Neurosci 25:10420–10436.

Kaas JH (1993) The functional organization of somatosensory cortex in primates. Ann Anat 175:509–518.

Kahn I, Pascual-Leone A, Theoret H, Fregni F, Clark D, Wagner AD (2005) Transient disruption of ventrolateral prefrontal cortex during verbal encoding affects subsequent memory performance. J Neurophysiol 94:688–698.

Kim JN, Shadlen MN (1999) Neural correlates of a decision in the dorsolateral prefrontal cortex of the macaque. Nat Neurosci 2:176–185.

Lebedev MA, Messinger A, Kralik JD, Wise SP (2004) Representation of attended versus remembered locations in prefrontal cortex. PLoS Biol 2:e365.

Levy R, Goldman-Rakic PS (2000) Segregation of working memory functions within the dorsolateral prefrontal cortex. Exp Brain Res 133:23–32.

Machens CK, Romo R, Brody CD (2005) Flexible control of mutual inhibition: a neural model of two-interval discrimination. Science 307:1121–1124.

Manoach DS, Greve DN, Lindgren KA, Dale AM (2003) Identifying regional activity associated with temporally separated components of working memory using event-related functional MRI. NeuroImage 20:1670–1684.

Mazurek ME, Roitman JD, Ditterich J, Shadlen MN (2003) A role for neural integrators in perceptual decision making. Cereb Cortex 13:1257–1269.

Miller EK (2000) The prefrontal cortex and cognitive control. Nat Rev Neurosci 1:59–65.

Miller P, Wang XJ (2006) From the cover: inhibitory control by an integral feedback signal in prefrontal cortex: a model of discrimination between sequential stimuli. Proc Natl Acad Sci USA 103:201–206.

Nelson AJ, Staines WR, McIlroy WE (2004) Tactile stimulus predictability modulates activity in a tactile-motor cortical network. Exp Brain Res 154:22–32.

Oldfield RC (1971) The assessment and analysis of handedness: the Edinburgh inventory. Neuropsychologia 9:97–113.

Pasternak T, Greenlee MW (2005) Working memory in primate sensory systems. Nat Rev Neurosci 6:97–107.

Petrides M, Pandya DN (1984) Projections to the frontal cortex from the posterior parietal region in the rhesus monkey. J Comp Neurol 228:105–116.

Postle BR (2006) Working memory as an emergent property of the mind and brain. Neuroscience 139:23–38.

Rizzolatti G, Luppino G (2001) The cortical motor system. Neuron 31:889–901.

Rizzolatti G, Fogassi L, Gallese V (2002) Motor and cognitive functions of the ventral premotor cortex. Curr Opin Neurobiol 12:149–154.

Roland PE (1981) Somatotopical tuning of postcentral gyrus during focal attention in man. A regional cerebral blood flow study. J Neurophysiol 46:744–754.

Romo R, Salinas E (2003) Flutter discrimination: neural codes, perception, memory and decision making. Nat Rev Neurosci 4:203–218.

Romo R, Brody CD, Hernandez A, Lemus L (1999) Neuronal correlates of parametric working memory in the prefrontal cortex. Nature 399:470–473.

Romo R, Hernandez A, Zainos A, Brody CD, Lemus L (2000) Sensing without touching: psychophysical performance based on cortical microstimulation. Neuron 26:273–278.

Romo R, Hernandez A, Zainos A, Lemus L, Brody CD (2002) Neuronal correlates of decision-making in secondary somatosensory cortex. Nat Neurosci 5:1217–1225.

Romo R, Hernandez A, Zainos A (2004) Neuronal correlates of a perceptual decision in ventral premotor cortex. Neuron 41:165–173.

Rowe JB, Passingham RE (2001) Working memory for location and time: activity in prefrontal area 46 relates to selection rather than maintenance in memory. NeuroImage 14:77–86.

Rowe JB, Toni I, Josephs O, Frackowiak RS, Passingham RE (2000) The prefrontal cortex: response selection or maintenance within working memory? Science 288:1656–1660.

Sakai K, Rowe JB, Passingham RE (2002) Active maintenance in prefrontal area 46 creates distractor-resistant memory. Nat Neurosci 5:479–484.

Salinas E, Hernandez A, Zainos A, Romo R (2000) Periodicity and firing rate as candidate neural codes for the frequency of vibrotactile stimuli. J Neurosci 20:5503–5515.

Sawaguchi T, Yamane I (1999) Properties of delay-period neuronal activity in the monkey dorsolateral prefrontal cortex during a spatial delayed matching-to-sample task. J Neurophysiol 82:2070–2080.

Schubotz RI, von Cramon DY (2001) Functional organization of the lateral premotor cortex: fMRI reveals different regions activated by anticipation of object properties, location and speed. Brain Res Cogn Brain Res 11:97–112.

Schubotz RI, von Cramon DY, Lohmann G (2003) Auditory what, where, and when: a sensory somatotopy in lateral premotor cortex. NeuroImage 20:173–185.

Schultz W (2000) Multiple reward signals in the brain. Nat Rev Neurosci 1:199–207.

Shadlen MN, Newsome WT (2001) Neural basis of a perceptual decision in the parietal cortex (area LIP) of the rhesus monkey. J Neurophysiol 86:1916–1936.

Smith EE, Jonides J, Marshuetz C, Koeppe RA (1998) Components of verbal working memory: evidence from neuroimaging. Proc Natl Acad Sci USA 95:876–882.

Staines WR, Graham SJ, Black SE, McIlroy WE (2002) Task-relevant modulation of contralateral and ipsilateral primary somatosensory cortex and the role of a prefrontal-cortical sensory gating system. NeuroImage 15:190–199.

Thees S, Blankenburg F, Taskin B, Curio G, Villringer A (2003) Dipole source localization and fMRI of simultaneously recorded data applied to somatosensory categorization. NeuroImage 18:707–719.

Tsutsui K, Jiang M, Sakata H, Taira M (2003) Short-term memory and perceptual decision for three-dimensional visual features in the caudal intraparietal sulcus (Area CIP). J Neurosci 23:5486–5495.

Wise SP, Boussaoud D, Johnson PB, Caminiti R (1997) Premotor and parietal cortex: corticocortical connectivity and combinatorial computations. Annu Rev Neurosci 20:25–42.

Zatorre RJ, Evans AC, Meyer E (1994) Neural mechanisms underlying melodic perception and memory for pitch. J Neurosci 14:1908–1919.